Quality factors in single-defect photonic-crystal lasers with asymmetric cladding layers

Cheolwoo Kim, Woo Jun Kim, Andrew Stapleton, Jiang-Rong Cao, John D. O'Brien, and P. Daniel Dapkus

Department of Electrical Engineering/Electrophysics, University of Southern California, Los Angeles, California 90089-0271

Received August 31, 2001; revised manuscript received January 9, 2002

We present quality factors of single-defect photonic-crystal resonant cavities with asymmetric cladding layers. The resonators studied here are dielectric slabs patterned with two-dimensional photonic crystals on a sapphire substrate. Three-dimensional finite-element and finite-difference time-domain routines were used to analyze the electromagnetic properties of these cavities. We observe that high quality factors (~800) can be obtained in these cavities for reasonable structures with thick enough dielectric slabs. This work was motivated by the need to place photonic-crystal resonators on a substrate to improve heat dissipation in photonic-crystal lasers. © 2002 Optical Society of America

OCIS codes: 140.0140.

Photonic-crystal microcavity lasers are potentially attractive optical sources in future communication systems. They have several advantages such as lithographically defined wavelengths[1] and expected low operating powers. Much work remains to be done, however, for these sources to find mainstream applications. Single-defect photonic-crystal lasers were first demonstrated in pulsed mode at low temperatures.[2] Room-temperature pulsed operation has since been demonstrated in lasers with larger mode volumes,[1,3–6] and continuous wave (cw) room-temperature operation has been reported in a photonic-crystal laser with a fusion-bonded substrate that had a layer that was subsequently converted to Al_xO_y.[7] The cw demonstration used a large hexagonal cavity formed in a triangular lattice. Continuous wave operation of single-defect photonic-crystal lasers, however, has not been reported to date. To operate such a laser at room temperature, it is necessary to design a high-Q (quality factor) resonant cavity that dissipates heat well. Poor heat dissipation is likely the major factor preventing cw operation of single-defect lasers in undercut device geometries. As in the cw operation of larger photonic-crystal cavities, a strategy for improving heat dissipation in single defect cavities is to wafer bond the semiconductor membrane containing the two-dimensional photonic crystal to a low-index-of-refraction, high-thermal-conductivity substrate. Here we choose sapphire as the substrate material. This complicates the electromagnetic design, however. There are two major effects of adding a uniform substrate below the photonic-crystal membrane. First, the presence of a substrate breaks the symmetry of the structure about the midplane of the device. This removes the ability to classify modes as either even or odd and removes the bandgap in the guided modes of the membrane.[8] Second, the substrate also will increase optical losses in the cavity because of the larger radiation loss into the substrate compared with an air-clad structure. Here we investigate the quality factor of these resonators as a function of the semiconductor membrane thickness. We will show that it is possible to obtain high-Q resonant cavities by increasing the membrane thickness while maintaining the in-plane mode localization. A significant complication occurs, however, when the slab becomes thick enough to support multiple modes. The multiple slab modes close the bandgap in the guided modes.[8,9] This introduces radiation loss in the in-plane direction. We analyze single-layer and multiple-layer dielectric slabs as a function of the slab thickness and compare the calculated threshold material gain required to achieve lasing in a single-defect cavity for each case. As an aside, we note that it should also be possible to obtain high-Q resonant cavities in the presence of a substrate if the in-plane mode localization is relaxed, but this issue is not pursued here.

Electromagnetic modes in purely two-dimensional photonic crystals can be classified as having either TE or TM polarization. TE modes have the electric field polarized in the plane of periodicity and TM modes have the magnetic field polarized in the plane of periodicity. Once the photonic crystal becomes finite in height, this classification scheme is lost. For example, in the original photonic-crystal laser demonstration,[2] the modes were not purely TE or TM. That demonstration, however, had inversion symmetry about the midplane of the device because the cladding layers were symmetric. This symmetry allows a classification of the modes as being even or odd about the midplane. At the midplane, the even mode is TE and the odd mode is TM, but away from that plane this TE or TM classification is no longer valid. In a cavity with symmetric cladding layers there is a gap formed for the even guided modes as well as for the odd guided modes. The bandgaps in the even and odd mode spectrum do not completely overlap, but since the two sets of modes are orthogonal there is still a gap for each mode classification. A sapphire substrate breaks the symmetry and there is no way to classify the modes of the cavity. As a result there is no longer a gap in the guided mode spectrum of the dielectric membrane. This has the po-

Report Documentation Page

Form Approved
OMB No. 0704-0188

1. REPORT DATE	2. REPORT TYPE	3. DATES COVERED
01 JUN 2005	**N/A**	**-**

4. TITLE AND SUBTITLE	5a. CONTRACT NUMBER
Quality factors in single-defect photonic-crystal lasers with asymmetric cladding layers	5b. GRANT NUMBER
	5c. PROGRAM ELEMENT NUMBER
6. AUTHOR(S)	5d. PROJECT NUMBER
	5e. TASK NUMBER
	5f. WORK UNIT NUMBER
7. PERFORMING ORGANIZATION NAME(S) AND ADDRESS(ES)	8. PERFORMING ORGANIZATION REPORT NUMBER
Department of Electrical Engineering-Electrophysics, University of Southern California, Los Angeles, CA 90089 USA	
9. SPONSORING/MONITORING AGENCY NAME(S) AND ADDRESS(ES)	10. SPONSOR/MONITOR'S ACRONYM(S)
	11. SPONSOR/MONITOR'S REPORT NUMBER(S)

12. DISTRIBUTION/AVAILABILITY STATEMENT
Approved for public release, distribution unlimited

13. SUPPLEMENTARY NOTES
See also ADM001923.

14. ABSTRACT

15. SUBJECT TERMS

16. SECURITY CLASSIFICATION OF:			17. LIMITATION OF ABSTRACT	18. NUMBER OF PAGES	19a. NAME OF RESPONSIBLE PERSON
a. REPORT	b. ABSTRACT	c. THIS PAGE			
unclassified	**unclassified**	**unclassified**	**UU**	**5**	

tential to limit or even eliminate the ability to obtain in-plane localization for a mode formed by a defect in the two-dimensional photonic-crystal lattice.

A more severe problem associated with the sapphire cladding is increased radiation loss into the sapphire. The radiation loss out of the plane of the photonic crystal is predicted to be the dominant optical loss in the demonstrated single-defect photonic-crystal-membrane laser structures. This loss arises because part of the optical mode is not totally internally reflected at the semiconductor–air interfaces at the top and bottom of the resonant cavity. In other words, the localization of the mode in real space causes a spread of the mode in wave-vector space, and a portion of the mode lies above the light line in k space.[9–12] This means that the mode is not completely guided by the membrane. This problem will become worse in a structure bonded to a sapphire substrate because the light line of the substrate has a lesser slope than the light line in an air-clad structure. This reduces the separation between the mode in k space, which is centered about the M point and the light line.

Figure 1 shows the geometry of the resonant cavity. Figure 2 shows the calculated band structure for both the symmetric air-clad and the asymmetric air–sapphire-clad photonic-crystal membranes. These calculations were performed by a finite-element analysis. Whitney 1 forms were used as vector basis functions in the finite-element calculation. The mesh density used was 2948 tetrahedral elements per cubic lattice constant. The symmetric air-clad structure consisted of a three-layer dielectric membrane surrounded by air. The membrane core had an index of refraction of 3.4 and a thickness of $0.2a$, where a is the lattice constant. The dielectric cladding layers on both sides of the core had a thickness of $0.1a$ and an index of 3.1. The ratio r/a was 0.3, where r is the radius of the holes. The air–sapphire-clad structure had the same dielectric membrane structure but with a sapphire layer below the membrane with an index of refraction of 1.6. The dielectric slab supports only a single mode at this thickness. The calculations illustrate the effects on the radiation mode condition when a substrate is used as a cladding layer. A larger optical loss results for the same membrane and photonic-crystal lattice compared with the symmetric air-clad geometry. There is also a shift in the bands from the air-clad structure to the sapphire substrate structure and a reduction in the band-gap. This occurs because for the same membrane thickness, the modes in the sapphire-bonded structure have a larger effective index. This results in a slight lowering of the mode frequency. The air band has a larger frequency reduction than the dielectric band, resulting in the gap reduction.

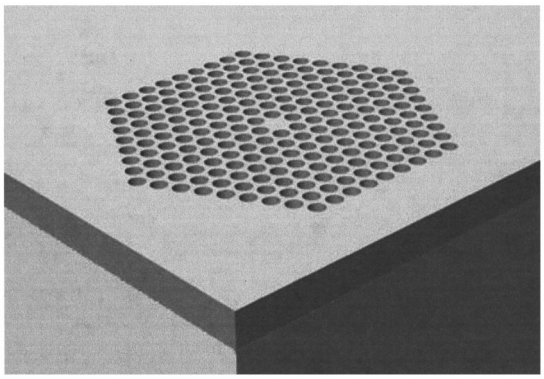

Fig. 1. Illustration of resonant cavity geometry modeled in this work.

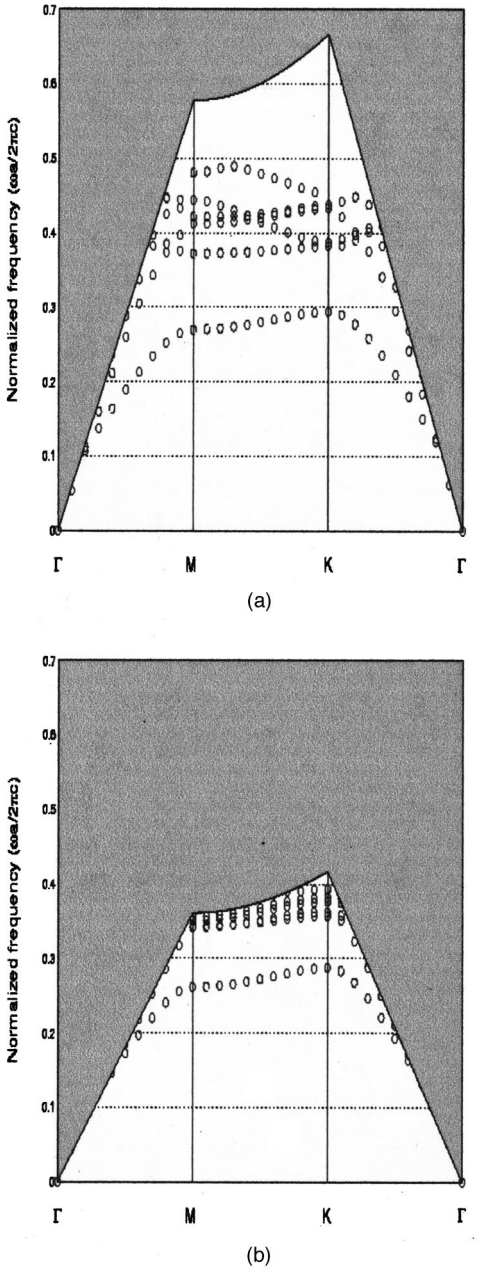

Fig. 2. Finite-element calculations of the dispersion relations of the photonic-crystal membrane for (a) Symmetric air cladding, (b) asymmetric air–sapphire cladding.

Figure 3 shows a cross-sectional view of the electric field intensity inside a photonic-crystal cavity bonded to sapphire. The figure was obtained from a three-dimensional finite-difference time-domain (FDTD) simulation. The FDTD calculations used a rectangular mesh with 25 points per lattice constant. The figure clearly shows an increase in the radiation loss into the substrate compared to the radiation loss into the air above. This

increased loss will significantly reduce the Q of the resonant cavity.

The quality factors of the resonator were calculated by using the FDTD code.[10,13–15] Here we are considering a triangular lattice with a single missing hole, and it is the Q of the doubly-degenerate donor-resonant mode associated with this missing hole that we are concerned with. The Q of the cavity was obtained by multiplying the resonant frequency, which is obtained from a Fourier transform of the field, by the energy stored in the cavity and then dividing by the power lost out of the cavity. Following Ref. 10, we can separate this Q into a Q due to radiation loss out the top of the cavity, Q_{top}; radiation loss into the sapphire, Q_{bottom}; and radiation loss in plane out of the photonic crystal, Q_{side}. In our calculations, the power radiated in plane was calculated by integrating the normal component of the Poynting vector over the four sidewalls of the calculation domain. The height of these walls was 5 d/a, where d is the dielectric slab thickness and a is again the photonic lattice constant. The angle at which power radiated was divided into vertical radiation, and in-plane radiation therefore varies slightly with d/a. This does not significantly affect the results, however. The reciprocal total Q is just the sum of the reciprocal component Qs. This total Q was verified by comparing the result of the Q obtained from the time rate of change of the energy in the resonant cavity.

Figure 4 shows the calculated Q_{side}, Q_{bottom}, and total Q as a function of the slab thickness. As noted above, $r/a = 0.3$, and seven lattice periods on each side of the defect were included. Figure 4(a) shows the data for a three-layer dielectric slab on sapphire, and Fig. 4(b) shows the data for a single-layer dielectric slab with a refractive index of 3.4 on sapphire. The membrane that was considered in Fig. 4(a) was an InGaAsP core of refractive index 3.4 with InP cladding on both sides, which had an index of refraction of 3.2. The figure shows that large Q values can be obtained for thick membranes. As expected, Q_{bottom} increases as the slab thickness increases. Q_{bottom} will be limited in practice by the maximum obtainable etch depth. It should also be expected that Q_{bottom} depends on r/a. Figure 5 shows the calculated Q_{top} and Q_{bottom} for a fixed membrane thickness of $d/a = 1$ as a function of r/a. The corresponding values for a symmetric air-clad structure are included for comparison. The Q values for the symmetric structure included in Fig. 5 are for radiation loss into the top (or bottom, but not both) in order to simplify the comparison with the sapphire-bonded structure. As expected, the radiation loss into the sapphire is larger than the radiation loss into the air for both the symmetric air-clad and sapphire-bonded resonant cavities. Figures 4(a) and 4(b) also show that for thick dielectric slabs the total Q of the cavity is not dominated by Q_{bottom} at all, but by Q_{side}. To obtain the maximum value of Q in the cavity, there is therefore an important trade-off between Q_{bottom} and Q_{side}. This occurs

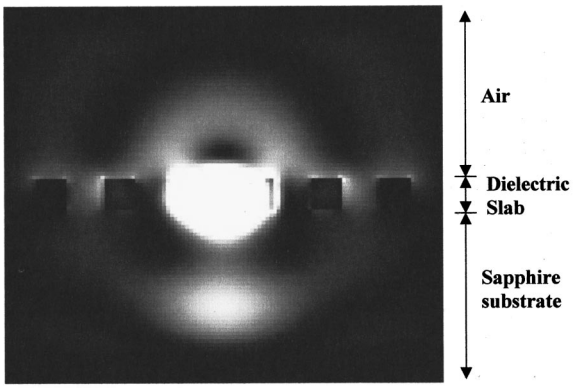

Fig. 3. FDTD calculation of electric field intensity inside the air–sapphire-clad photonic-crystal resonant cavity.

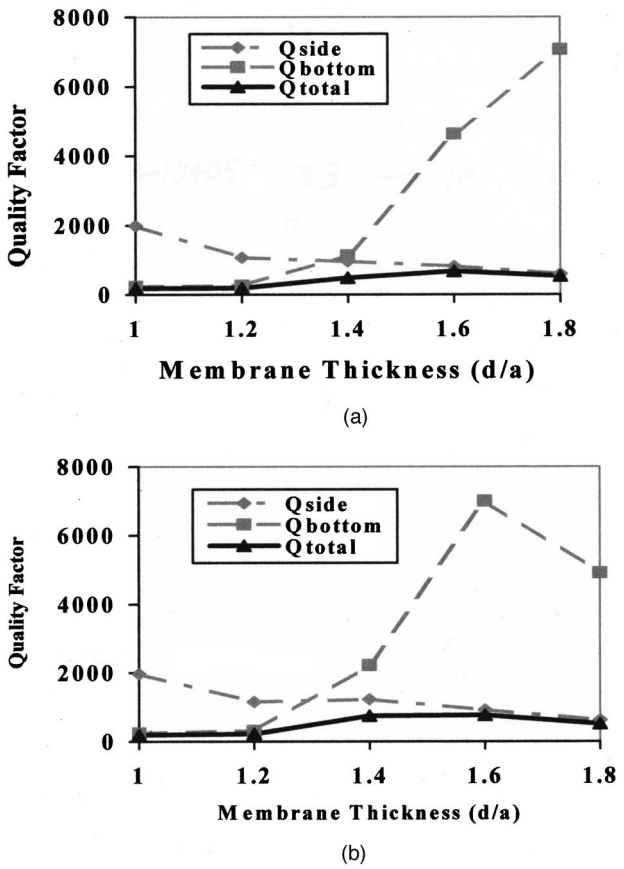

Fig. 4. FDTD calculation of Q_{bottom}, Q_{side}, and Q_{total} as a function of the membrane thickness for (a) three-layer slab on sapphire, (b) single-layer slab on sapphire.

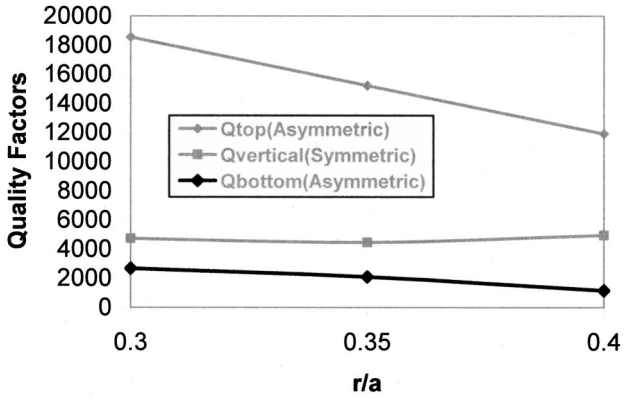

Fig. 5. FDTD calculation of Q_{top}, Q_{vertical} and Q_{bottom} as a function of r/a with the membrane thickness fixed at 1.6 a.

because as the thickness of the dielectric slab increases, it supports more modes. These modes close what would be a gap in the guided modes of the slab if the slab were symmetric. From Fig. 4(a) and 4(b) we see that Q_{side} decays slightly more rapidly with increasing slab thickness for the three-layer slab than it does for the single-layer slab. This is true because the higher-order slab modes are spaced farther apart in frequency for the three-layer slab than they are for the single-layer slab. This has the effect of closing the gap more quickly.

Figures 4 and 5 illustrate the fact that good vertical confinement can be obtained in sapphire-bonded photonic-crystal resonant cavities by increasing the membrane thickness and choosing the r/a ratio carefully. We also found that Q_{side} is a strong function of the slab thickness, so d/a must be chosen carefully.

We also checked that the in-plane confinement was not affected by the asymmetric cladding of the sapphire. We plot in Fig. 6 the Q_{side}, Q_{top}, Q_{bottom}, and total Q values as a function of the number of photonic-crystal lattice periods for a membrane thickness of $0.85a$ and an r/a value of 0.3. This membrane supports a single mode. The figure shows that the Q_{side} values increase rapidly as the number of lattice periods increases, until the total Q is dominated by the out-of-plane losses. It is important to remember, however, that Q_{side} becomes limited owing to the closing of the bandgap as d/a increases. This closing of the bandgap with increasing d/a is not a result of the asymmetry introduced by the sapphire layer, and we have therefore chosen to consider conditions in Fig. 6 that illustrate the effects of the asymmetry more simply. Since this in-plane loss does not saturate in Fig. 6 with increasing number of lattice periods, there appears to be no evidence of significant coupling between the confined resonant mode and the band edge states that correspond to those bands that have odd symmetry in the air-clad geometry. We expect that as the membrane thickness increases, the influence of the sapphire cladding on the resonant electromagnetic mode decreases, since the thickness of the InP cladding layer between the InGaAsP waveguide core and the sapphire layer is increasing. As the InP layer thickness increases to infinity, the modes become even and odd modes of the InGaAsP–InP semiconductor layer structure.

Finally, we calculated the threshold material gain required for these single defect resonant cavities. As

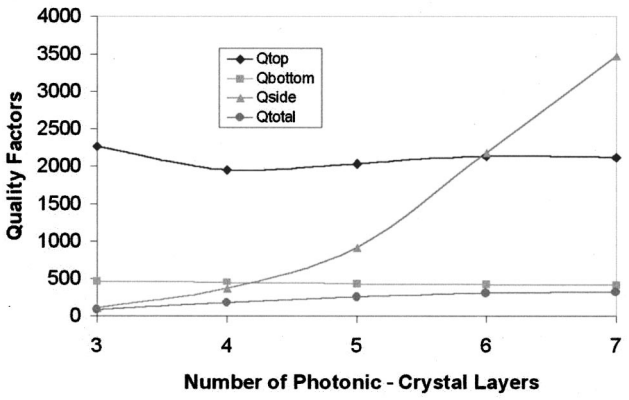

Fig. 6. FDTD calculation of Q values as a function of the number of photonic-crystal periods for a single-mode slab.

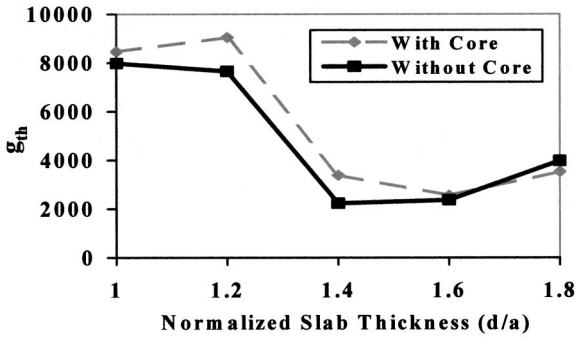

Fig. 7. FDTD calculation of threshold modal gain as a function of d/a for the three-layer and single-layer slab cases.

shown in Figs. 4(a) and 4(b), the single-layer slab has a larger total Q value than the three-layer slab for the same slab thickness. A laser design must also account for the confinement factor, however, which is larger for the three-layer dielectric slab than it is for the single-layer structure. Figure 7 shows the calculated threshold material gain versus d/a for each of the two slab configurations. This was obtained using the relation

$$Q = \omega t_{\text{ph}} = \frac{2\pi n_{\text{eff}}}{\lambda}\frac{1}{\Gamma g_{\text{th}}},$$

where Γ is the confinement factor, n_{eff} is the effective modal index, and g_{th} is the threshold material gain. This model considers only radiation losses, of course. Γ was calculated for the resonant mode by using the FDTD code. The vertical confinement factor was calculated over a region of 40 nm at the center of the dielectric slab. 40 nm corresponds to two grid points at this mesh density. The in-plane confinement factor was taken to be approximately 1. We see that there is a tradeoff between Q and the confinement factor and that the lowest threshold gain condition occurs for a single-layer slab at $d/a = 1.4$. This is not necessarily the maximum Q value, but the maximum value of the product ΓQ. We note that a material gain value of 2200 cm^{-1} for four quantum well's, is a reasonable value for this material system.[16] At $d/a = 1.4$, finite-difference calculations indicate that the dielectric slab supports two modes: the fundamental mode and a second mode that has approximate odd symmetry about the midpoint of the slab. The radiative coupling into this higher-order mode will be very small in a laser with a quantum well active region near the center of the slab because the confinement factor for this mode is very small.

We show that high-Q single-defect photonic-crystal resonant cavities can be formed by bonding a semiconductor membrane to a high-thermal-conductivity sapphire substrate. The increased radiation loss into the sapphire can be compensated for by increasing the semiconductor membrane thickness. There are trade-offs, however, between Q_{bottom} and Q_{side} as the slab thickness increases. We see no effects of the asymmetry in the in-plane Q. Finally, there is an additional trade-off between the confinement factor and the total Q value in designing a laser cavity.

ACKNOWLEDGMENTS

This work was supported in part by the U.S. Army Research Laboratory and the U.S. Army Research Office under contract DAAD19-99-1-0121 and by the Defense Advanced Research Projects Agency under contracts MDA 972-00-1-0019 and N00014-00-C-8079.

C. Kim may be reached by e-mail at cheolwoo@usc.edu.

REFERENCES

1. O. Painter, A. Husain, A. Scherer, P. Lee, I. Kim, J. D. O'Brien, and P. D. Dapkus, "Lithographic tuning of a photonic crystal laser array," IEEE Photonics Technol. Lett. **12**, 1126–1128 (2000).
2. O. Painter, R. K. Lee, A. Scherer, A. Yariv, J. D. O'Brien, P. D. Dapkus, and I. Kim, "Two-dimensional photonic bandgap defect mode laser," Science **284**, 1819–1821 (1999).
3. O. Painter, A. Husain, A. Scherer, J. D. O'Brien, I. Kim, and P. D. Dapkus, "Room temperature photonic crystal defect lasers at near-infrared wavelengths in InGaAsP," J. Lightwave Technol. **17**, 2082–2088 (1999).
4. J. K. Hwang, H. Y. Ryu, D. S. Song, I. Y. Han, H. W. Song, H. K. Park, and Y. H. Lee, "Room-temperature triangular-lattice two-dimensional photonic band gap lasers operating at 1.54 μm," Appl. Phys. Lett. **76**, 2982–2984 (2000).
5. P. T. Lee, J. P. Cao, S. J. Choi, J. D. O'Brien, and P. D. Dapkus, "Room temperature operation of VCSEL-pumped photonic crystal lasers," submitted to IEEE Photonics Technol. Lett. (2001).
6. C. Monat, C. Seassal, X. Letartre, P. Viktorovitch, P. Regreny, M. Gendry, P. Rojo-Romeo, G. Hollinger, E. Jalaguier, S. Pocas, and B. Aspar, "InP 2D photonic crystal microlaser on Si wafer: room temperature operation at 1.55 μm," Electron. Lett. **37**, 764–765 (2001).
7. J. K. Hwang, H. Y. Ryu, D. S. Song, I. Y. Han, H. K. Park, D. H. Jang and Y. H. Lee, "Continuous room-temperature operation of optically pumped two-dimensional photonic crystal lasers at 1.6 μm," IEEE Photonics Technol. Lett. **12**, 1295–1297 (2000).
8. S. G. Johnson, S. Fan, R. Villeneuve, J. D. Joannopoulos, and L. A. Kolodzeijski, "Guided modes in photonic crystal slabs," Phys. Rev. B **60**, 5751–5758 (1999).
9. P. R. Villeneuve, S. Fan, S. G. Johnson, and J. D. Joannopoulos, "Three-dimensional photon confinement in photonic crystals of low-dimensional periodicity," IEE Proc. Optoelectron. **145**, 384–390 (1998).
10. O. Painter, J. Vuckovic, and A. Scherer, "Defect modes of a two-dimensional photonic crystal in an optically thin dielectric slab," J. Opt. Soc. Am. B **16**, 275–284 (1999).
11. H. Benisty, D. Labilloy, C. Weisbuch, C. J. M. Smith, T. F. Krauss, D. Cassagne, A. Beraud, and C. Jouanin, "Radiation losses of waveguide-based two-dimensional photonic crystals: positive role of the substrate," Appl. Phys. Lett. **76**, 532–534 (2000).
12. S. G. Johnson, S. Fan, A. Mekis, and J. D. Joannopoulos, "Multipole-cancellation mechanism for high-Q cavities in the absence of a complete photonic bandgap," Appl. Phys. Lett. **78**, 3388–3390 (2001).
13. Z. Bi, Ying Shen, Keli Wu, and J. Litva, "Fast finite-difference time domain analysis of resonators using digital filtering and spectrum estimation techniques," IEEE Trans. Microwave Theory Tech. **40**, 869–872 (1992).
14. C. T. Chan, Q. L. Yu, and K. M. Ho, "Order-N spectral method for electromagnetic waves," Phys. Rev. B **51**, 16635–16642 (1995).
15. E. Miyai and K. Sakoda, "Quality factor for localized defect modes in a photonic crystal slab upon a low-index dielectric substrate," Opt. Lett. **26**, 740–742 (2001).
16. A. Mathur and P. D. Dapkus, "Fabrication, characterization and analysis of low threshold current density 1.55 mm strained quantum-well lasers," IEEE J. Quantum Electron. **32**, 222–226 (1996).